

Lysosomal iron recycling in mouse macrophages is dependent upon both LcytB and Steap3 reductases

Fanjing Meng, Brittany A. Fleming, Xuan Jia, Alexis A. Rousek, Matthew A. Mulvey, and Diane M. Ward

Department of Pathology, University of Utah School of Medicine, University of Utah, Salt Lake City, UT

Key Points

- Lysosomal reductase activity is necessary for iron release and recycling.
- Loss of lysosomal reductases increases the proliferation of intracellular pathogens.

Iron that is stored in macrophages as ferritin can be made bioavailable by degrading ferritin in the lysosome and releasing iron back into the cytosol. Iron stored in ferritin is found as Fe^{3+} and must be reduced to Fe^{2+} before it can be exported from the lysosome. Here we report that the lysosomal reductase Cyb561a3 (LcytB) and the endosomal reductase six-transmembrane epithelial antigen of prostate 3 (Steap3) act as lysosomal ferrireductases in the mouse macrophage cell line RAW264.7 converting Fe^{3+} to Fe^{2+} for iron recycling. We determined that when lysosomes were loaded with horse cationic ferritin, reductions or loss of LcytB or Steap3 using CRISPR/Cas9-mediated knockout technology resulted in decreased lysosomal iron export. Loss of both reductases was additive in decreasing lysosomal iron export. Decreased reductase activity resulted in increased transcripts for iron acquisition proteins DMT1 and transferrin receptor 1 (Tfrc1) suggesting that cells were iron limited. We show that transcript expression of *LcytB* and *Steap3* is decreased in macrophages exposed to *Escherichia coli* pathogen UTI89, which supports a role for these reductases in regulating iron availability for pathogens. We further show that loss of LcytB and Steap3 in macrophages infected with UTI89 led to increased proliferation of intracellular UTI89 suggesting that the endolysosomal system is retaining Fe^{3+} that can be used for proliferation of intravesicular pathogens. Together, our findings reveal an important role for both LcytB and Steap3 in macrophage iron recycling and suggest that limiting iron recycling by decreasing expression of endolysosomal reductases is an innate immune response to protect against pathogen proliferation and sepsis.

Introduction

Iron plays an essential role in enzymatic reactions that drive heme, iron-sulfur cluster, lipid, and DNA synthesis.^{1,2} The majority of total body iron (3-4 g) can be found as hemoglobin in red blood cells (2-3 g). Red blood cells have a life span of ~100 to 120 days necessitating a mechanism for iron recycling from senescent red cells.³ Macrophages play a central role in iron recycling from senescent or damaged red cells by delivering about 20 to 30 mg of iron back into the bloodstream daily for further rounds of utilization.^{4,5} Macrophages in the liver and spleen engulf most of the aged red cells, and the resulting phagosome fuses with the lysosome where the red cell is degraded. As the red blood cell is degraded, heme released into the lysosomal lumen is then transported out of the lysosome by HRG1.^{6,7} Cytosolic heme is catabolized by heme oxygenase-1 releasing Fe^{2+} into the cytosol that can then be exported out of macrophages through ferroportin (Fpn) or stored in cytosolic ferritin.^{8,9} Under iron-limited conditions, ferritin in the

Submitted 24 June 2021; accepted 16 December 2021; prepublished online on *Blood Advances* First Edition 4 January 2022; final version published online 14 March 2022. DOI 10.1182/bloodadvances.2021005609.

Requests for data sharing may be submitted to Diane M. Ward diane.mcveyward@path.utah.edu.

The full-text version of this article contains a data supplement.

© 2022 by The American Society of Hematology. Licensed under Creative Commons Attribution-NonCommercial-NoDerivatives 4.0 International (CC BY-NC-ND 4.0), permitting only noncommercial, nonderivative use with attribution. All other rights reserved.

macrophages can be engulfed in an autophagosome through recruitment of the cargo receptor NCOA4,¹⁰⁻¹² which then fuses with the lysosome.¹³ In the lysosome, ferritin is broken down, and Fe³⁺ is released into the lysosomal lumen where it can be stored or transported back into the cytosol through divalent metal transport 1 (DMT1), Natural resistance-associated macrophage protein 1 (NRAMP1) or transient receptor potential mucopolin 1 (TRPML1).^{14,15} Because iron transporters identified to date accept Fe²⁺ only as a substrate, there must be a mechanism to convert lysosomal Fe³⁺ to Fe²⁺ before it can be exported to the cytosol. To date, a mammalian lysosomal ferrireductase has not been described for macrophage iron recycling. One candidate that is predicted to be a macrophage lysosomal ferrireductase is Cyb561a3 (referred to here as LcytB), which has been localized to lysosomes in the RAW264.7 mouse macrophage cell line, although its function as a reductase for iron was not demonstrated.¹⁶ LcytB is a member of the cytochrome b561 (Cyt b561) family, which is a group of intrinsic membrane proteins involved in ascorbate-mediated transmembrane electron transport.¹⁷ An example of a Cyt b561 reductase is Dcytb, which acts in iron absorption in the gut converting Fe³⁺ to Fe²⁺ for iron import at the apical surface of the gut epithelium.¹⁸ *Saccharomyces cerevisiae* also expresses plasma membrane ferrireductases Fre1 and Fre2, and the absence of both results in poor growth on iron-limited media.¹⁹ The poor growth of $\Delta fre1\Delta fre2$ yeast can be partially complemented by overexpression of mammalian LcytB, but this complementation requires plasma membrane localization of LcytB,²⁰ whereas LcytB is localized to lysosomes in macrophages.¹⁶ A recent article showed that transcripts for the gene encoding LcytB (*Cyb561a3*) were dramatically increased when lysosomal acidification was blocked and that this increase was a result of cellular iron limitation.²¹ This suggests that LcytB is important in iron release from lysosomes, although this has not been directly shown.

The six-transmembrane epithelial antigen of prostate 3 (Steap3) is an endosome-localized ferrireductase that works with DMT1 to export iron out of the endosome.²² Previous studies have shown that Steap3 partner transporter DMT1 translocates to the lysosome upon ferritin loading,¹⁴ which suggests that Steap3 may also translocate to the lysosome of macrophages depending upon iron status and reductase need. Here we report that both LcytB and Steap3 are important in lysosomal iron release from macrophages. We generated deletions in *LcytB*, *Steap3*, and in both in RAW264.7 mouse macrophages. We show that preloading the lysosome with iron-laden horse spleen cationic ferritin (CF) (which is broken down in the lysosome) and iron is then released to the cytosol, which results in increased endogenous mouse cytosolic ferritin levels; the absence of LcytB or Steap3 decreases the release of lysosomal iron. We also show that the absence of both reductases is additive in iron release from lysosomes. We determined that Steap3 shows increased colocalization with the lysosomal marker Lamp2 when cells are fed CF. Finally, we show that loss of these reductases in RAW264.7 cells increases the proliferation of *Escherichia coli* pathogen UTI89, which can live in the lysosome, confirming that more iron is bioavailable for the survival and proliferation of vacuolar pathogens.

Materials and methods

Cell culture

The murine macrophage cell line RAW264.7 was cultured in Dulbecco's modified Eagle medium (DMEM; Mediatech) containing 0.2

mM L-alanyl-L-glutamine dipeptide (Gibco), 0.1 mM sodium pyruvate (Sigma), 10% fetal bovine serum, and penicillin-streptomycin (Sigma) at 37°C under 5% CO₂. For ascorbate experiments, cells were incubated with 0.3 M ascorbate for 48 hours after CF loading. C57BL/6 bone marrow-derived macrophages were isolated and grown as previously described.²³

Bone marrow-derived macrophages and RNA interference

C57BL/6 bone marrow-derived macrophages were isolated and grown as previously described.²³ Small interfering RNA (siRNA) pools matching selected regions of *LcytB* complementary DNA (cDNA) sequences and a random sequence pool were purchased from Thermo Fisher Scientific. Transfections were performed on bone marrow-derived macrophages plated at 50% confluence using electroporation (Amaxa Neon) with siRNA pools at a final concentration of 100 nm according to manufacturer's directions. Cells were transfected twice (time 0 and time 24 hours) and then grown for an additional 48 to 72 hours before harvesting for quantitative reverse transcriptase polymerase chain reaction (qRT-PCR) or ferritin measurements.

CRISPR/Cas9 generation and complementation of mutations

LcytB and/or *Steap3* mutants were generated by using a lentiviral CRISPR/Cas9 system. CRISPR constructs were generated under the guidance of Crystal Davey, PhD, Core Director, Mutation Generation Detection Core. The *LcytB*-CRISPR constructs were targeted to the sequence on exon 3 or exon 4 of the mouse *cyb561a3*, whereas the *Steap3*-CRISPR constructs were targeted to a sequence on exon 1 of the mouse *Steap3*. Reductase mutants were identified by high-resolution melting analysis, and changes in *Cyb561a3* or *Steap3* messenger RNA (mRNA) were confirmed by qRT-PCR. For *LcytB* complementation, the pCMV3-GFPspark-human *cyb561a3* plasmid (Sino Biological) was transfected into *LcytB* mutants using the Neon electroporation transfection system (Thermo Fisher Scientific) according to the manufacturer's protocol for macrophages. The transfected cells with green fluorescent protein (GFP) were selected for analysis by flow cytometry (BD FACSAria) and kept in hygromycin 200 µg/mL for 2 weeks. For *Steap3* complementation, the pCDNA6-Steap3-Myc-His construct (a generous gift from Mark Fleming, MD, Harvard University)²² was transfected into *Steap3* mutants using the same transfection system as described above. The transfected cells were selected in 10 to 20 µg/mL blasticidin. All selected *LcytB* or *Steap3* overexpression cell lines were then placed in antibiotic-free media to confirm stable expression before complementation analysis and to ensure that any observed effects were not the result of the presence of antibiotics.

qRT-PCR

Total RNA was harvested using the RNeasy Mini Kit (QIAGEN) according to the manufacturer's protocol. A High Capacity cDNA Reverse Transcription Kit (Applied Biosystems) and 2 µg RNA were used to make cDNA. Power SYBR Green Master Mix (Applied Biosystems) was used on a Mastercycler Realplex2 system (Eppendorf). Actin was used as a control housekeeping gene. The $\Delta\Delta Ct$ method was used to compare the variation of transcripts among samples. Specificity and efficiency were checked before using this method. Primers for mouse genes included *Actin* forward

5'-GACGGCCAAGTCATCACTATTG-3', *Actin* reverse 5'-CCA-CAGGATTCCATACCCAAGA-3', *LcytB* forward 5'-CGAGAATC GCACACCTCTACTC-3', *LcytB* reverse 5'-TTTCAGGAGGCTTC GCAGCCAC-3', *Steap2* forward 5'-GAGCAACGCTTTGAACTG-GAGAG-3', *Steap2* reverse 5'-GGCAAGAACGAAGTTTGGTGGT G-3', *Steap3* forward 5'-TCTTCAGCACCGCCAGTCTAAC-3', *Steap3* reverse 5'-CTGGCTGATCACTGCAGATGAG-3', *Steap4* forward 5'-GGGAATCACTTCCTTGCCATCAG-3', *Steap4* reverse 5'-TCCGCCATACACCAAAGTGTGG-3', *DMT1* forward 5'-TTGC AGCGAGACTTGGAGTGGT-3', *DMT1* reverse 5'-GCTGAGCCA ATGACTTCCTGCA-3', transferrin receptor 1 (*Tfrc1*) forward 5'-GAAGTCCAGTGTGGGAACAGGT-3', *Tfrc1* reverse 5'-CAAC-CACTCAGTGGCACCAACA-3', *Fpn* forward 5'-CCATAG TCTCTGTGAGCCTGCT-3', *Fpn* reverse 5'-CTTGCAACTGT GTCACCGT-3',

Membrane isolation and western blot

Cells were harvested, washed twice in phosphate-buffered saline (PBS), and then resuspended in 2 mL buffer (0.25 M sucrose, 10 mM Trizma base, and 0.5 mM tetrasodium EDTA [pH 7.4]). Cells were homogenized using a ball-bearing homogenizer with a 0.2561-inch diameter ball. The homogenates were centrifuged at 400g at 4°C for 5 minutes, and the supernatant was centrifuged at 14 000g at 4°C for 30 minutes. The pellet was solubilized in lysis buffer (1% Triton, 150 mM NaCl, 0.5 mM tetrasodium EDTA, and 10 mM Trizma base [pH 7.4]) containing 2× protease inhibitors (Roche) and incubated for 30 minutes on ice; the lysate was centrifuged at 14 000g at 4°C for 30 minutes. The membrane lysates with 1× Laemmli buffer were boiled at 100°C for 10 minutes, run on a 4% to 20% sodium dodecyl sulfate-polyacrylamide gel electrophoresis (SDS-PAGE) Tris-glycine gel (Bio-Rad) at 100V for 60 to 90 minutes in buffer (25 mM Tris, 192 mM glycine, 0.1% SDS), and transferred to nitrocellulose membranes (GE Healthcare Life Sciences) at 100V for 1 hour in Western transfer buffer (25 mM Tris, 192 mM glycine, 20% v/v methanol). Membranes were blocked at 37°C for 30 minutes in TBST (150 mM NaCl, 3 mM KCl, 28 mM Tris, 0.1% Tween 20) with 10% milk and washed extensively. Membranes were probed with primary antibodies Steap3 (rabbit, 1:400; Abcam, ab104654), 6XHis (rabbit, 1:1000; Abcam, ab9108), VDAC1 (rabbit, 1:1000; Abcam, ab154856), or Lamp2 (rat, 1:250; Developmental Hybridoma, GL2A7) overnight at 4°C in TBST 10% milk. Membranes were washed extensively and incubated in a 1:5000 dilution of peroxidase-conjugated goat anti-rabbit or donkey anti-rat antibodies at 37°C for 60 minutes. Western blots were developed using Western Lightning reagent (Perkin-Elmer). Blots were quantified using Fiji ImageJ software.

Measurement of cytosolic ferritin

RAW264.7 cells (2.5×10^5) were seeded in 4 mL DMEM and grown for 48 hours. At 48 hours, cells were incubated with or without 80 µg horse spleen CF (Sigma) for 60 minutes and then washed with cold Hanks balanced salt solution (HBSS). Four mL fresh DMEM media was added, and cells were grown for an additional 48 hours as described.²⁴ Cells were washed with cold HBSS, lysed in lysis buffer, and incubated on ice for 30 minutes; lysates were centrifuged at 14 000g at 4°C for 30 minutes. A bicinchoninic acid (BCA) assay (Thermo Fisher Scientific) was used for protein determination, and ferritin levels were measured by using a mouse ferritin enzyme-linked immunosorbent assay (ELISA; Immunology Consultants Laboratory) according to the manufacturer's

instructions. All experiments were repeated a minimum of 3 times with 4 biological replicates per cell type. Ferritin levels were also assessed in wild-type (WT), mutant *LcytB* #2, *LcytB* #2 expressing WT *LcytB*, or reductase mutant *LcytBY66A* expressed by lentiviral transduction²⁵ (a generous gift from Ben Gewurz, MD) using the mouse ferritin ELISA assay.

Immunofluorescence microscopy

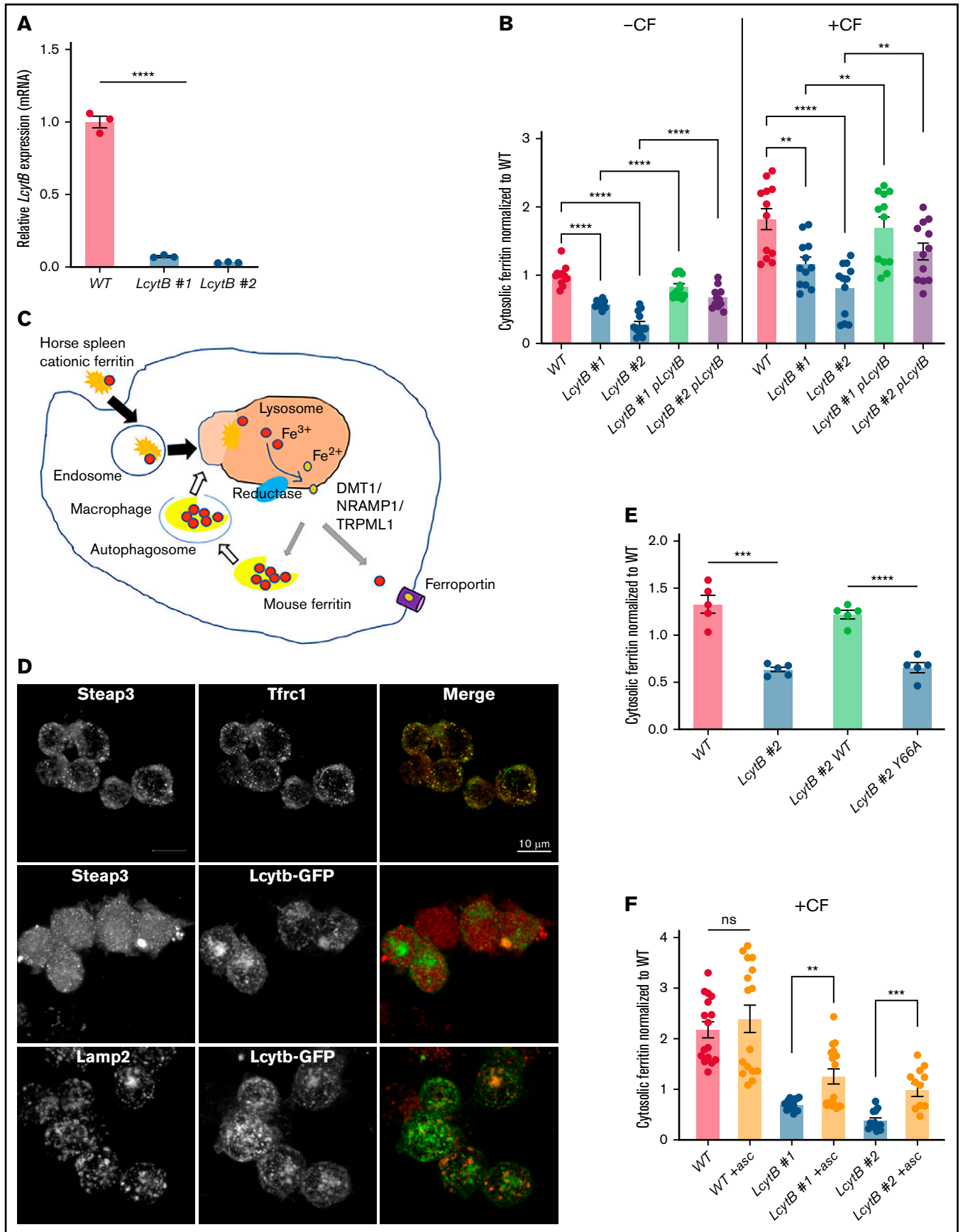
RAW264.7 cells were plated on glass coverslips, incubated with or without CF as described above, fixed in 3.7% formaldehyde/PBS at room temperature for 20 minutes, permeabilized in 0.1% saponin/PBS/1% bovine serum albumin, and incubated with rat anti-mouse LAMP2 (1:200) and rabbit anti-Steap3 (1:100) at 4°C overnight. Then cells were extensively washed and incubated in secondary antibody Alexa488-conjugated goat anti-rat immunoglobulin G (IgG) (1:750) or Alexa594-conjugated goat anti-rabbit IgG (1:750) at room temperature for 1 hour. Coverslips were mounted onto glass slides and images were captured using a Zeiss 700 Confocal Microscope (z series, 0.6-micron step) with a ×60 oil immersion lens with a ×1.4 aperture. Images were processed as .tiff files in Adobe Photoshop, and colocalization was assessed with the assistance of staff from the University of Utah Cell Imaging Core. For other colocalization studies, RAW264.7 cells with or without the pCMV3-GFPspark-human Cyb561a3 plasmid (*LcytB*-GFP) were processed as above and incubated with anti-Steap3 (1:100) and rat anti-Tfrc1 (1:100), rabbit anti-Steap3 (1:100) and mouse anti-GFP (1:500), or rabbit anti-GFP (1:500) and rat anti-mouse LAMP2 (1:200) antibodies. Secondary antibodies used for these samples included Alexa594-conjugated goat anti-rabbit IgG (1:750) for Steap3, Alexa594-conjugated goat anti-rabbit IgG (1:750) for LAMP2, Alexa488-conjugated goat anti-mouse IgG (1:750) for Tfrc1 and GFP, and Alexa488-conjugated goat anti-rabbit IgG (1:750) for GFP.

E. coli invasion and proliferation assays

Invasion and cell association assays were performed as previously described by Eto et al.²⁶ Briefly, within 24 hours of seeding into 24-well plates, confluent monolayers of host cells were infected with UTI89 at a multiplicity of infection of 5 to 10 bacteria per host cell. Plates were spun at 600g for 5 minutes to expedite and synchronize bacterial contact with the host cell monolayers before incubation at 37°C in the presence of 10 µg/mL gentamycin, which prevents replication but does not kill bacteria. Cells were washed extensively at 4°C and the amount of macrophage-associated bacteria was determined. Cells were then incubated for 30 minutes (T_0) or with an additional overnight incubation (T_{ON}) in medium containing the host membrane-impermeable bactericidal agent gentamicin (100 µg/mL) (Sigma-Aldrich). Host cells were then washed 3 times with PBS²⁺ (PBS supplemented with Mg²⁺/Ca²⁺) and lysed in 1 mL of PBS²⁺ containing 0.3% Triton X-100. Bacterial titers from the lysates were determined by serial dilution and plating on Luria-Bertani (LB) agar plates. The experiment was repeated 5 times with 2 biological replicates per cell type.

Statistical analyses

All experiments were performed a minimum of 3 times unless otherwise stated. Statistical tests were performed using Prism8 software. Student *t* test analysis was used for comparison between 2 groups. *P* values ≤ .05 were considered statistically significant. Outlier



analyses were performed on all graphs using either Grubbs or ROUT tests ($Q = 1.0$) as recommended by Prism software. Identified outliers were removed from the plots and before the statistical analyses.

Results

Loss of *LcytB* resulted in reduced lysosomal iron export

Iron released from ferritin that is degraded in the lysosome is Fe^{3+} must be converted to Fe^{2+} to be exported, because all identified mammalian iron transporters transport divalent metals. This conversion requires the presence of a reductase on the lysosome. Previous studies have suggested that *LcytB* might be that reductase. To determine whether *LcytB* is the macrophage lysosomal reductase responsible for the conversion of Fe^{3+} to Fe^{2+} and subsequent lysosomal iron export, we used the mouse macrophage cell line RAW264.7 and CRISPR/Cas9 targeted mutagenesis of *Cyb561a3*, which encodes *LcytB*. We targeted either exon 3 or exon 4 of *Cyb561a3*, hereinafter referred to as *LcytB*. We identified 2 clones, *LcytB* #1 and *LcytB* #2, that have significantly reduced levels of *LcytB* transcripts (Figure 1A). Unfortunately, commercially available *LcytB* antibodies did not work for assessing *LcytB* protein levels in mouse samples. Both *LcytB* #1 and *LcytB* #2 showed a slower growth rate compared with WT cells (supplemental Figure 1A). These results suggest that *LcytB* may be important in regulating bioavailability of iron for proliferation. One measure of cellular iron status is cytosolic ferritin levels. To determine whether loss of *LcytB* affected cellular iron levels, we measured endogenous ferritin levels. When the cells were maintained under normal growth conditions, clones *LcytB* #1 and *LcytB* #2 had significantly lower endogenous ferritin compared with WT cells (Figure 1B, -CF). These results suggested that *LcytB* contributes to maintaining endogenous ferritin levels in macrophages. To determine whether the loss of *LcytB* affected iron release and recycling from lysosomes, we took advantage of a previously established method to load lysosomes with CF and measure iron release from lysosomes.²⁴ This method uses horse spleen CF, which is taken up by fluid-phase endocytosis and delivered to the lysosome where it is degraded, and ferritin iron is either stored in the lysosome or transported into the cytosol (Figure 1C). The released iron is then either exported out of the cell through ferroportin or is incorporated into

newly synthesized cytosolic ferritin for storage. Importantly, the horse spleen CF is not recognized by antibodies against mouse ferritin that are part of the ELISA assays used to measure cellular mouse ferritin.²⁴ Using CF allows us to distinguish between steady-state endogenous cytosolic ferritin and increases in ferritin synthesis upon lysosomal iron release. Indeed, loading with CF increased endogenous cytosolic ferritin levels in WT cells approximately twofold, whereas *LcytB* mutants showed a 50% to 70% reduction in cytosolic ferritin compared with CF-fed WT cells (Figure 1B, +CF). We confirmed that reductions in endogenous ferritin in *LcytB*-mutant cells were not a consequence of decreased fluid-phase endocytosis, which is required for CF uptake. Cells were incubated with fluorescently labeled Alexa594-dextran (10 000 molecular weight), and total fluorescence was determined using flow cytometry at the indicated time points. No differences were seen in the rate or amount of dextran taken up in WT vs *LcytB*-mutant cells (supplemental Figure 1B). This supports the notion that reductions in *LcytB* affect iron export out of lysosomes but not fluid-phase endocytosis.

To confirm that the changes in endogenous ferritin were a result of the loss of *LcytB* and not because of some other compensatory mutation in our CRISPR/Cas9 clones, we transfected *LcytB*-mutant cells with a plasmid containing a GFP-tagged human *LcytB* whose expression was driven by a cytomegalovirus (CMV) promoter. Previous studies have shown that overexpressed *LcytB* localizes with Lamp2 and LysoTracker-positive compartments reflecting late endosomes and lysosomes.¹⁶ We confirmed expression using immunofluorescence microscopy and showed that *LcytB*-GFP colocalizes with Lamp2, but not with endosomal reductase Steap3 (Figure 1D). We note that not all *LcytB*-GFP localizes with Lamp2. We speculate that this is because of overexpression and that *LcytB*-GFP may still be in the synthesis/secretory pathway enroute to lysosomal localization. *LcytB*-GFP⁺ cells were sorted by flow cytometry, maintained in hygromycin to establish stable cell lines, and expanded in the absence of hygromycin for further use in ferritin assays. *LcytB*-mutant cells overexpressing *LcytB*-GFP showed increased levels of endogenous ferritin both with and without CF loading (Figure 1B, p*LcytB* (plasmid expressing WT human *LcytB*-GFP)), providing strong evidence that the reduction in endogenous ferritin levels seen in our mutant cell lines was the result of loss of *LcytB* and was not

Figure 1. CRISPR/Cas9-mediated mutation of *LcytB* in RAW264.7 macrophages results in decreased iron release from lysosomes. (A) qRT-PCR analysis was performed on WT and mutants *LcytB* #1 and *LcytB* #2 generated by using *LcytB* and *Actin* (control) primers. Data were normalized to the WT level of 1.0 ($n = 3$ biological replicates). (B) WT, mutants *LcytB* #1 and *LcytB* #2, and mutants *LcytB* #1 and *LcytB* #2 expressing WT human *LcytB*-GFP were grown in tissue culture medium supplemented with or without 20 μ g/mL horse CF for 1 hour, washed extensively, and grown for an additional 48 hours in growth medium. Cells were then lysed, and endogenous mouse ferritin levels were measured. Data were normalized to a WT cytosolic ferritin level of 1.0 (-CF) ($n \geq 6$ biological replicates). p*LcytB* represents the plasmid for WT human *LcytB*-GFP. (C) A model of CF uptake, lysosomal breakdown, iron release, and endogenous ferritin iron storage. The macrophage takes up horse spleen CF by endocytosis and delivers it to the lysosome (black arrows). CF is degraded in the lysosome, and Fe^{3+} is converted to Fe^{2+} by an unknown reductase (blue oval). Iron is exported out of the lysosome into the cytosol by divalent metal transporters DMT1, NRAMP1, or TRPML1. Cytosolic iron can be exported out through ferroportin or incorporated into newly synthesized cytosolic ferritin (gray arrows) for storage. Upon increased iron demand, cytosolic ferritin is engulfed by autophagy (white arrows), the autophagosome fuses with the lysosome, Fe^{3+} released from degraded ferritin is reduced, and Fe^{2+} is exported from the lysosome. (D) WT or WT cells that overexpress pCMV*LcytB*-GFP were fixed and stained for Steap3 and Tfrc1, Steap3 and GFP, or Lamp2 and GFP, and images were captured. Representative confocal images are shown with single channels and merged (red/green) images are indicated ($n = 3$ biological replicates). (E) WT, mutant *LcytB* #2, mutant *LcytB* #2 expressing WT human *LcytB*, and *LcytB* reductase mutant Y66A²⁵ were lysed, and endogenous mouse ferritin levels were determined as in panel B ($n = 5$ biological replicates). (F) WT and mutants *LcytB* #1 and *LcytB* #2 were incubated with CF (as in panel B) and were grown in the presence or absence of 0.3 M ascorbate (asc) for 48 hours; endogenous ferritin levels were determined as in panel B. Data were normalized to the WT cytosolic ferritin level of 1.0 (-CF) ($n \geq 6$ biological replicates). More information on procedures is provided in "Materials and methods." Error bars represent standard error of the mean (SEM). ** $P < .01$; *** $P < .001$; **** $P < .0001$. ns, not significant.

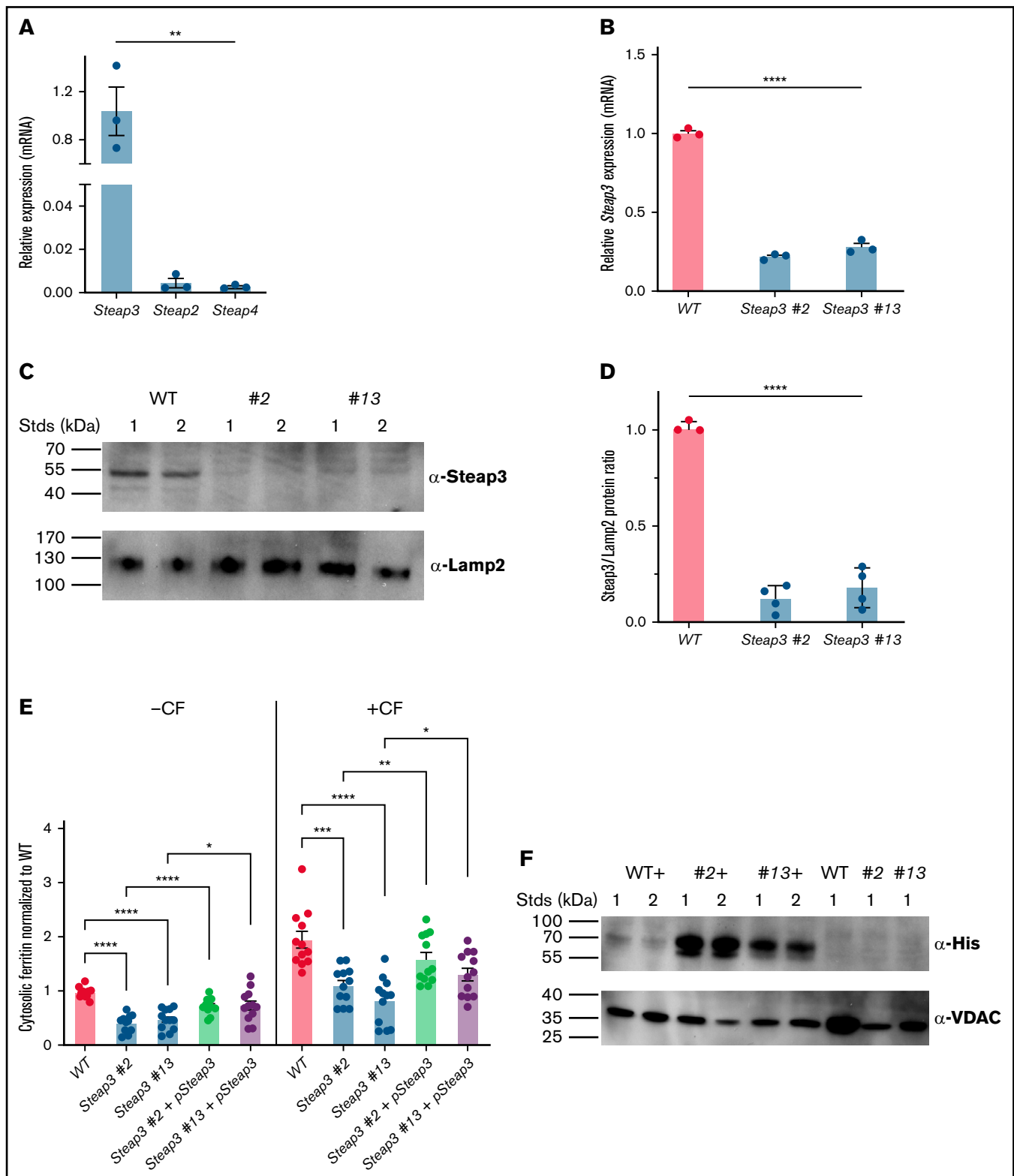


Figure 2. Loss of Steap3 in macrophages results in decreased release of iron from lysosomes. (A) RNA was isolated from WT RAW264.7 cells, cDNA was generated, and qRT-PCR was performed for *Steap2*, *Steap3*, *Steap4*, and *Actin*. Data were normalized to a *Steap3* level of 1.0 (ratio *Steap3:Actin*; n = 3 biological replicates). (B) RNA was isolated from WT, *Steap3* #2, and *Steap3* #13 cells, cDNA was generated, and qRT-PCR was performed for *Steap3* and *Actin*. Data were normalized to a WT level of 1.0 (n = 3 biological replicates). (C) Membranes were isolated from biological replicates of WT, *Steap3* #2, and *Steap3* #13 cells, and western blot analysis was performed for Steap3 and Lamp2. A representative blot with 2 biological replicates is shown. Stds, standard molecular mass markers. (D) Western blots were quantified using Fiji Image J with Lamp2 as a loading control. Data were normalized to a WT level of 1.0 (n = 4 biological replicates). (E) WT, mutants *Steap3* #2 and *Steap3* #13, and *Steap3* mutants

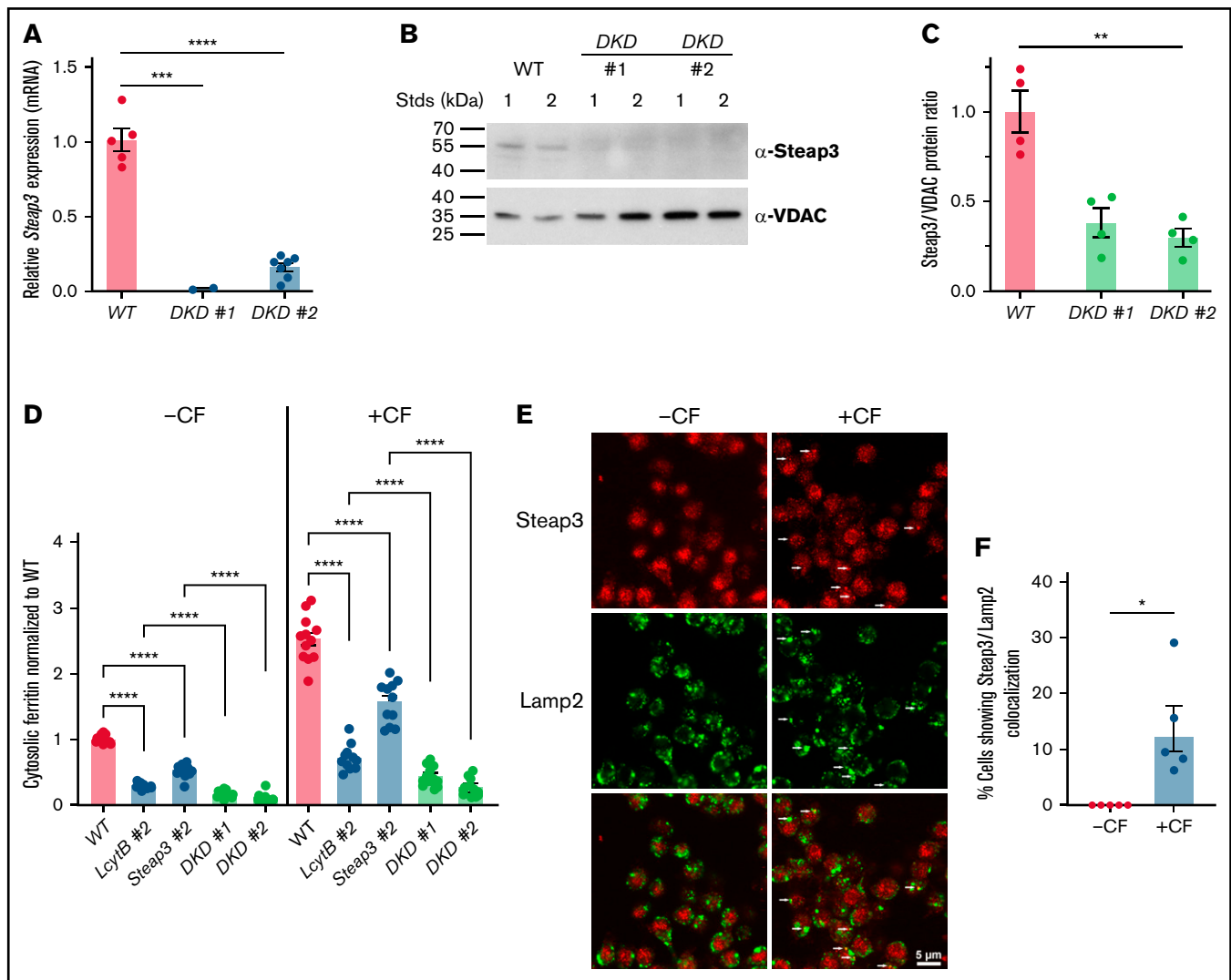


Figure 3. Loss of LcytB and Steap3 is additive in limiting the export of lysosomal iron. (A) *Steap3* was mutated in *LcytB* #2 as described in Figure 2. qRT-PCR analysis was performed on WT and *DKD* #1 and *DKD* #2 clones using *Steap3* and *Actin* primers. Data were normalized to a WT level of 1.0. ($n > 3$ -7 biological replicates). (B) Crude membrane preparations were performed for WT, *DKD* #1, *DKD* #2, and *Steap3* #2, and western blot analysis for Steap3 and VDAC was performed. VDAC was used as a membrane loading control. A representative blot with 2 biological replicates is shown. (C) Western blots were quantified using Fiji Image J using VDAC as a membrane loading control. Data were normalized to a WT level of 1.0 ($n = 4$ biological replicates). (D) Cytosolic ferritin levels were determined in cells incubated in the presence or absence of CF as in Figure 2B. Data were normalized to a WT cytosolic ferritin level (-CF) of 1.0 ($n \geq 6$ biological replicates). (E) WT cells were treated with or without CF as in Figure 1B and fixed. Steap3 and Lamp2 localization were detected by confocal immunofluorescence microscopy. A representative field is shown for -CF +CF. Arrows denote areas of Steap3 and Lamp2 colocalization in CF-loaded cells. (F) Data from 5 biological replicate slides were quantified, and the data were displayed as percentage of cells showing Steap3 and Lamp2 colocalization. More information on procedures is provided in "Materials and methods." Error bars represent SEM. * $P < .05$; ** $P < .01$; *** $P < .001$; **** $P < .0001$.

a result of off-target CRISPR/Cas9-generated mutations. We also determined that, although WT *LcytB* improves endogenous ferritin levels in the mutant *LcytB* #2 cell line, the Y66A-mutant *LcytB* reductase does not (Figure 1E).

Previous studies using overexpression in yeast have shown that *LcytB* is a reductase, and reductase activity was increased when yeast were provided exogenous ascorbate.²⁰ Earlier studies also showed that addition of ascorbate to fibroblasts increased

Figure 2. (continued) expressing WT human Steap3-His were grown in tissue culture medium supplemented with or without 20 $\mu\text{g}/\text{mL}$ horse CF for 1 hour, washed extensively, and grown for an additional 48 hours in growth medium. Cells were then lysed, and endogenous mouse ferritin levels were measured. Data were normalized to a WT cytosolic ferritin level of 1.0 (-CF) ($n \geq 6$ biological replicates). (F) Membranes were isolated from cells as in panel E, and Steap3-His levels were determined by western blot. Voltage-dependent anion channel (VDAC) levels were used as a membrane loading control. A representative blot with 2 biological replicates of complemented cells is shown. More information on procedures is provided in "Materials and methods." Error bars represent SEM. * $P < .05$; ** $P < .01$; *** $P < .001$; **** $P < .0001$.

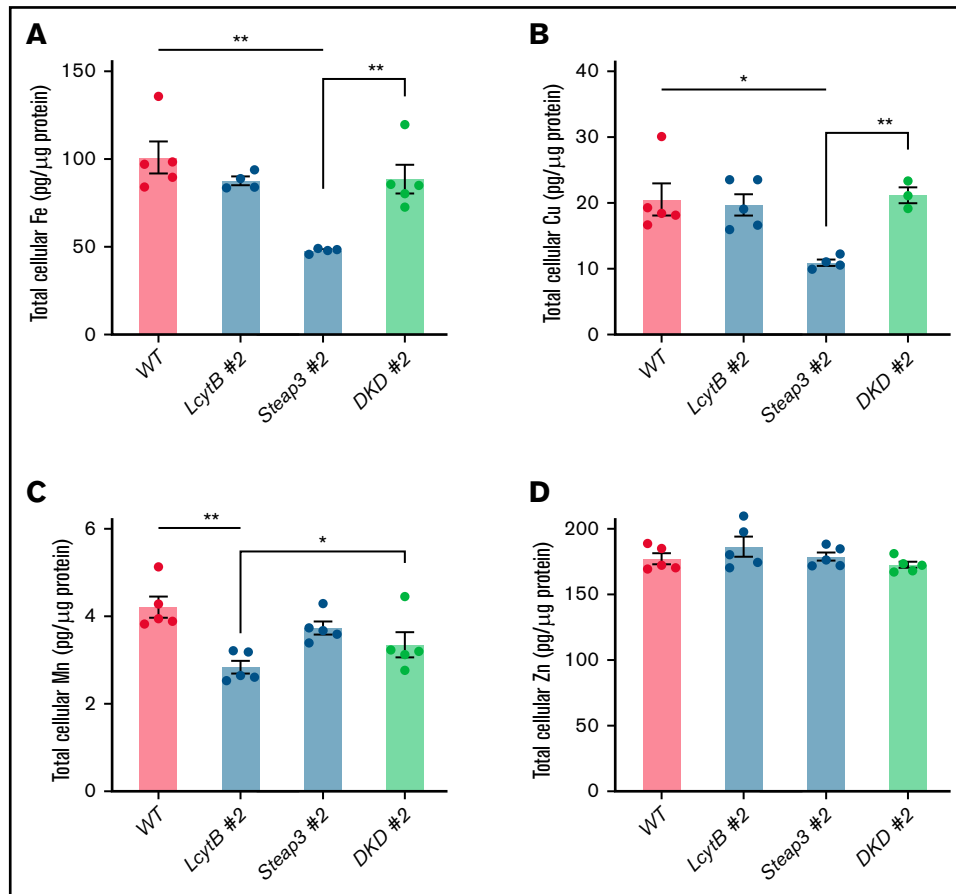


Figure 4. Loss of LcytB or Steap3 alters total levels of cellular metals. Metal levels were determined in WT, *LcytB* #2, *Steap3* #2, and *DKD* #2 cells using ICP-MS. Graphs represent 3 to 5 biological replicates for whole cells. Data were normalized to protein levels (pg/μg protein). Fe (A), Cu (B), Mn (C), and Zn (D). * $P < .05$; ** $P < .01$.

lysosomal iron export, which suggests that ascorbate was limiting for reductase activity.²⁴ Ascorbate dependence has not been shown in macrophages. Surprisingly, the addition of ascorbate to WT RAW264.7 macrophages did not significantly affect ferritin levels in cells fed CF (Figure 1F). This result suggests that LcytB in macrophages is not an ascorbate-dependent reductase or that in the context of the lysosome, there is another electron donor that is available for reduction of Fe³⁺. We anticipated that loss of LcytB would prevent any ascorbate-dependent increases in cytosolic ferritin in CF-fed cells; however, our *LcytB* mutants showed increased cytosolic ferritin levels upon the addition of ascorbate. One possible explanation for this result is that ascorbate directly reduces Fe³⁺, making it available for transport into cells and out of lysosomes.

To determine whether loss of LcytB affects primary macrophage iron release from lysosomes, we knocked down *LcytB* in primary C57BL/6 bone marrow-derived macrophages using siRNA. However, we were able to reduce *LcytB* transcripts only by about 25% to 30%, which unfortunately did not result in changes in endogenous ferritin levels (supplemental Figure 1C). We tried using lentiviral CRISPR/Cas9 technology in bone marrow-derived macrophages as it has been previously described,²⁷ but we were unable to successfully transduce these primary cells in contrast to successfully transducing RAW264.7 cells.

Loss of Steap3 resulted in reduced export of lysosomal iron

Loss of LcytB decreased the ability to export iron from the lysosome as measured by reductions in endogenous ferritin synthesis. The decrease that resulted from LcytB loss, however, was not complete, because cells still showed increased cytosolic ferritin upon CF lysosome loading. This suggests that either there is some functional LcytB present on the lysosome or that there is another reductase that contributes to iron recycling from the lysosome. Our qRT-PCR results show that *LcytB* expression is dramatically reduced (>90%) in our mutant cells (Figure 1A), which makes this possibility less likely. We focused on the possibility of the presence of another lysosomal reductase. Steap3 is a reductase that is present in the endocytic pathway²² and is expressed by macrophages.²⁸ *Steap3*^{-/-} mice show abnormal iron homeostasis with increased anemia. However, the latter phenotype was attributed to endosomal iron export in red cell precursors.²⁹ We confirmed that *Steap3* is expressed in the RAW264.7 macrophage cell line, whereas the homologous reductases *Steap2* and *Steap4* showed low levels of expression (Figure 2A). To determine whether Steap3 is important in iron recycling from the macrophage lysosome, we used CRISPR/Cas9 targeted mutagenesis to create *Steap3*-mutant RAW264.7 cells. We successfully mutated *Steap3* and identified 2 clones, Steap3 #2 and

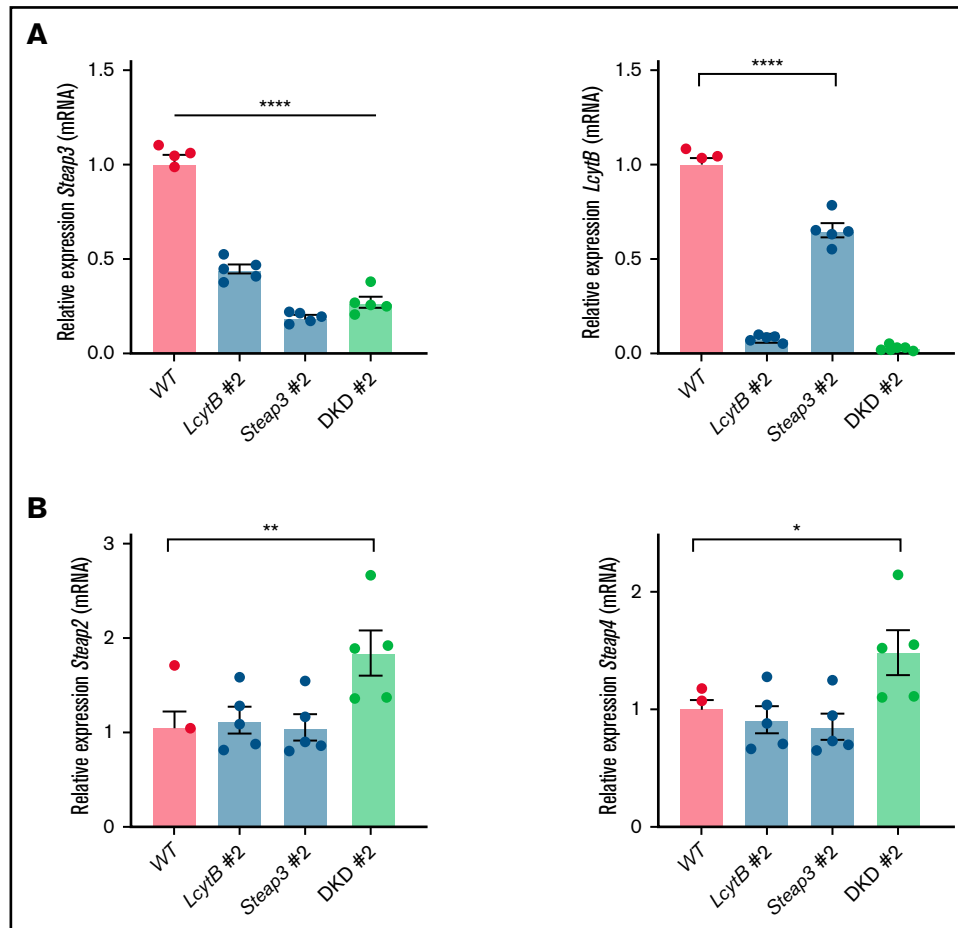


Figure 5. Loss of lysosomal reductases *LcytB* or *Steap3* affect the expression of other ferrireductases. (A) qRT-PCR was performed for *Steap3*, *LcytB*, and *Actin* from WT, *LcytB* #2, *Steap3* #2, and DKD #2. Data were normalized to the WT level of 1.0. (B) qRT-PCR was performed for *Steap2*, *Steap4*, and *Actin* from WT, *LcytB* #2, *Steap3* #2, and DKD #2 (n = 4-5 biological replicates). More information on procedures is provided in "Materials and methods." Error bars represent SEM. *P < .05; **P < .01; ****P < .0001.

Steap3 #13, with significantly reduced *Steap3* transcript levels (Figure 2B). Western blot analysis confirmed the presence of *Steap3* protein in WT RAW264.7 cells and dramatically reduced *Steap3* levels in selected *Steap3* mutants (*Steap3* #2 and *Steap3* #13; Figure 2C-D). *Steap3* mutants did not show any growth defect and may have a slight growth advantage compared with WT cells (supplemental Figure 2). *Steap3* mutants also did not show any defect in endocytosis (supplemental Figure 1B), but they had less endogenous cytosolic ferritin compared with control RAW264.7 cells grown under normal cell culturing conditions (Figure 2E, -CF). *Steap3* has previously been localized to endosomes and functions with DMT1 to reduce transferrin-delivered Fe^{3+} to Fe^{2+} for export from the endosome to the cytosol.³⁰ DMT1 has been shown to translocate from the endosome to the lysosome to export ferritin-released iron from the lysosome in hepatocytes when iron is limited by chelation treatment.¹⁴ To determine whether *Steap3* also functions as a lysosomal reductase, we incubated *Steap3* mutants and WT RAW264.7 cells with CF and measured endogenous ferritin level changes. When WT cells were incubated with CF, endogenous ferritin level increased as expected; however, the levels were significantly decreased in the *Steap3* mutants (Figure 2E, +CF). Complementation analysis confirmed that the change in iron release

from lysosomes was the result of reduced levels of *Steap3*, because overexpressing mouse *Steap3*-His expressed under a CMV promoter²² in *Steap3* mutant cells increased ferritin levels closer to those of WT cells. We confirmed *Steap3*-His expression (Figure 2F, WT+, *Steap3* #2+, *Steap3* #13+) and noted that *Steap3*-His expression was higher in the *Steap3* mutants (*Steap3* #2 and *Steap3* #13) compared with WT cells harboring the *Steap3*-His plasmid (WT+). This limited our ability to assess whether overexpression of *Steap3* improves the export of lysosomal iron. We speculate that there may be more selective pressure to keep *Steap3* in the mutant cell lines to control cellular iron levels. Our complementation results confirmed that the changes in ferritin levels in *Steap3* mutants were a result of the loss of *Steap3* and not an off-target effect of the CRISPR/Cas9-driven mutagenesis.

Loss of *LcytB* and *Steap3* is additive in reducing the export of lysosomal iron

Loss of either *LcytB* or *Steap3* reduced lysosome iron recycling by about 50%. We wondered whether these effects were additive. To answer this question, we mutated *Steap3* in *LcytB* #2 using the same CRISPR/Cas9 strategy that was used to generate single

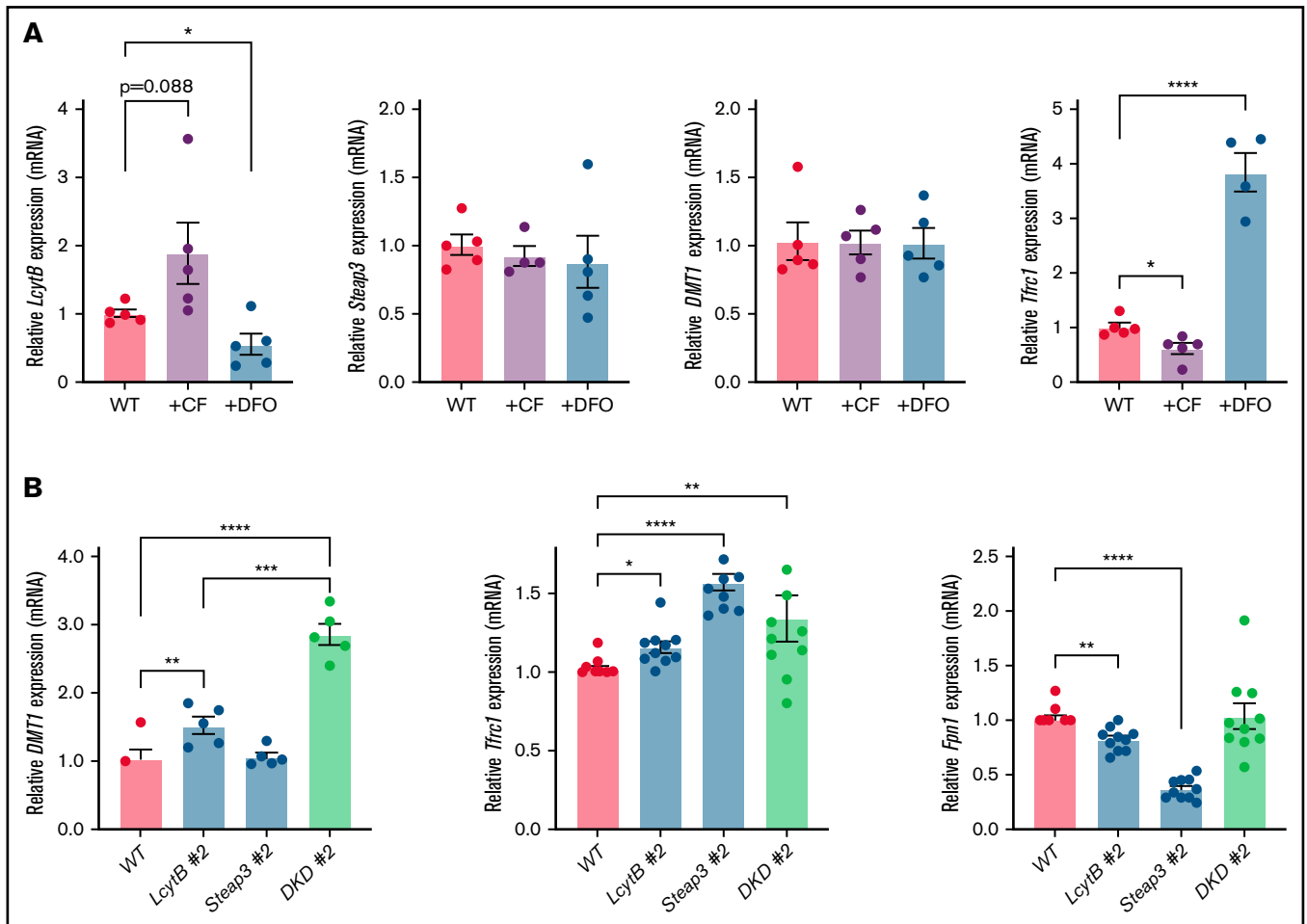


Figure 6. Loss of *LcytB* and *Steap3* alters iron acquisition transcripts. (A) WT cells were incubated with or without CF or grown in the presence or absence of DFO for 48 hours. qRT-PCR was performed for *LcytB*, *Steap3*, *DMT1*, *Tfrc1*, and *Actin*. Data are the ratio of *Actin* levels and are normalized to WT cells grown without CF or DFO as 1.0 ($n = 4$ or more biological replicates). (B) WT, *LcytB*-mutant, *Steap3*-mutant, and DKD cells were grown as in panel A and transcript levels for *DMT1*, *Tfrc1*, *Fpn1*, and *Actin* were measured using qRT-PCR. Data are the ratio of *Actin* levels and are normalized to WT cells under similar growth conditions (1.0) ($n = 4$ or more biological replicates). More information on procedures is provided in "Materials and methods." Error bars represent SEM. * $P < .05$; ** $P < .01$; *** $P < .001$; **** $P < .0001$.

Steap3 mutations and selected 2 double knockdown (DKD) clones, DKD #1 and DKD #2, as determined by qRT-PCR (Figure 3A). We confirmed that the DKD clones showed significant reductions in *Steap3* protein (Figure 3B-C). Loss of both *LcytB* and *Steap3* resulted in a significant growth defect compared with WT cells (supplemental Figure 3), suggesting that the cells are limited for iron. We examined whether the loss of both *LcytB* and *Steap3* affected iron release from CF breakdown in lysosomes compared with loss of *LcytB* or *Steap3* alone. DKD clones contained significantly less cytosolic ferritin compared with *LcytB* or *Steap3* mutants under normal cell culture conditions or when fed with CF (Figure 3D). Together, our results support that both *LcytB* and *Steap3* function as reductases that are important in the release of iron from lysosomes. Because *Steap3* has predominantly been ascribed to act in release of iron from endosomes,³¹ we wondered whether *Steap3* could translocate to the lysosome. To test this hypothesis, we examined *Steap3* localization in cells fed CF. If *Steap3* is working in the endosome, we would expect to see no change in *Steap3* localization upon CF lysosome loading. Conversely, if *Steap3* localized to the lysosome upon lysosome iron loading, we would expect to see

increased colocalization with the lysosomal marker Lamp2. Loading macrophages with CF resulted in increased colocalization of *Steap3* with Lamp2 (Figure 3E); however, not all cells showed increased *Steap3* colocalized upon CF loading (Figure 3F). Our data show that, similar to results reported for *DMT1*,¹⁴ some *Steap3* localizes to the lysosome, thus permitting iron reduction and transport into the cytosol.

Loss of *LcytB* or *Steap3* alters total levels of cellular metals

To determine whether the loss of *LcytB* or *Steap3* affects iron levels, we used inductively coupled plasma mass spectrometry (ICP-MS) with whole-cell lysates. We determined that loss of *Steap3*, but not *LcytB*, reduced levels of whole-cell iron (Fe) (Figure 4A). We suggest that whole-cell Fe levels are reduced in the *Steap3*-mutant cells because RAW264.7 cells are highly dependent upon $Tf(Fe)_2/Tfrc1/Steap3$ -mediated cellular iron uptake. We speculate that whole-cell iron levels are not altered by loss of *LcytB* because the iron becomes sequestered within the lysosome. Loss of *Steap3*

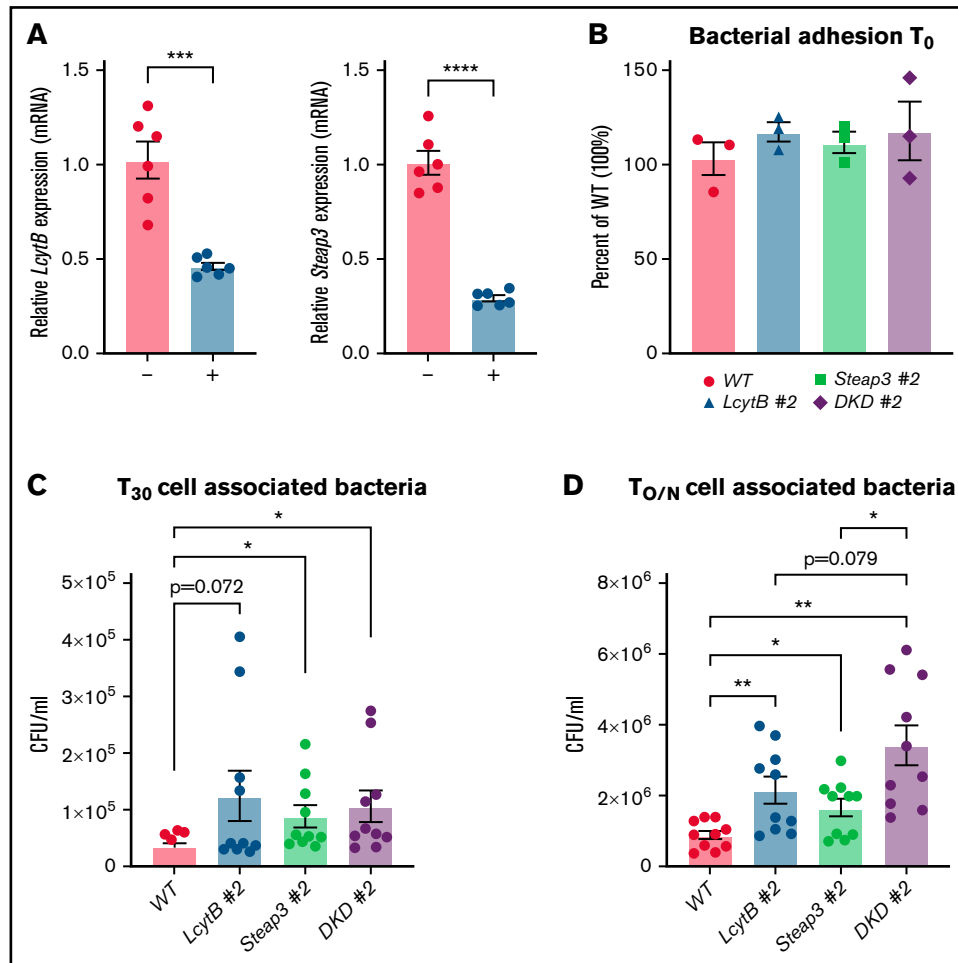


Figure 7. Loss of lysosomal reductases affects intracellular vesicular bacterial growth. (A) RNA was isolated from WT cells infected with UTI89 cells washed and incubated for 30 minutes followed by washing with 10 μ g/mL gentamicin (T_0), and qRT-PCR was performed using *LcytB*, *Steap3*, and *Actin* primers. Data were normalized to noninfected WT cells as 1.0 ($n = 6$ biological replicates). (B) WT, *Steap3* #2, *LcytB* 100-14, and DKD 120 were infected with UTI89, cells were washed in the presence of 10 μ g/mL gentamicin (T_0) ($n = 3$ biological replicates). The data are expressed as colony-forming units per milliliter (CFU/mL). (C) After gentamicin washing as in panel B, cells were incubated for 30 minutes and washed with gentamicin (T_{30}). (D) Cells were incubated overnight ($T_{0/N}$), washed in gentamicin, and lysed. Bacterial titers from cell lysates were determined ($n = 10$ biological replicates). More information on procedures is provided in "Materials and methods." Error bars represent SEM. * $P < .05$; ** $P < .01$; *** $P < .001$; **** $P < .0001$.

also reduced total cellular copper (Cu) levels (Figure 4B), whereas loss of *LcytB* reduced manganese (Mn) levels (Figure 4C). No changes in the amounts of zinc (Zn) were observed (Figure 4D). We do not know the reasons for these specific Cu and Mn changes in *Steap3* and *LcytB* mutants. Interestingly, the loss of both reductases resulted in recovery of WT whole-cell levels of Fe, Cu, and Mn. We speculate that this may be a result of upregulation of plasma membrane metal transporters in response to loss of both reductases as a means to meet cellular demands for these metals.

Loss of lysosomal reductases affects the expression of other ferrireductases

Macrophages express several reductases that can reduce multivalent metals. We examined whether the loss of *LcytB* or *Steap3* affected the expression other ferrireductases. We anticipated that some reductases may be upregulated in response to loss of *LcytB* or *Steap3*. Surprisingly, loss of *LcytB* decreased expression of

Steap3 (Figure 5A). Similarly, loss of *Steap3* decreased *LcytB* transcript levels. We determined that RAW264.7 cells express low levels of *Steap2* and *Steap4* (Figure 2A) compared with *LcytB* and *Steap3* levels, and these transcripts were unchanged by loss of either *LcytB* or *Steap3* (Figure 5B). However, both *Steap2* and *Steap4* expression were increased upon loss of both *LcytB* and *Steap3*. These results suggest that the expression of the endolysosomal localized reductases *LcytB* and *Steap3* are tightly coordinated. When those reductases are absent, macrophages increase the expression of other reductases to increase bioavailable iron, either through acquisition of external iron or release of iron from the endolysosomal system.

Loss of *LcytB* or *Steap3* alters iron acquisition gene expression

We hypothesized that *LcytB* levels might be affected by cellular iron levels, which we modified by either loading cells with

lysosomal iron or by growing cells under iron limitation using the iron chelator desferoxamine (DFO). qRT-PCR analysis showed that *LcytB* transcripts were increased when the lysosome was loaded with iron (CF loading) and decreased when cells were limited for iron by growth in DFO (Figure 6A). *Steap3* transcripts were unaffected by CF or DFO. Similar to *Steap3*, *DMT1* transcripts were unaffected. To ensure that the iron limitation and CF-loading growth conditions were changing cellular iron status, we measured transferrin receptor 1 (*Tfrc1*) transcripts. It is known that under iron-limited conditions, iron regulatory proteins 1 and 2 (IRP1 and IRP2) bind to the 3' untranslated regions of *Tfrc1* mRNA, which contain iron regulatory elements to stabilize the mRNA.³² As expected, CF-loading resulted in decreased *Tfrc1* transcripts, whereas iron limitation (DFO) dramatically increased *Tfrc1* transcripts. That *DMT1* expression was unchanged upon altered cellular iron levels in RAW264.7 macrophages confirms observations previously reported for the mouse macrophage cell line J774.³³ We wondered whether expression of these iron acquisition genes, *DMT1* and *Tfrc1*, was affected in our *LcytB*- and *Steap3*-mutant RAW264.7 cells. In response to loss of the reductase *LcytB*, *DMT1* transcripts levels were increased; however, no changes in *DMT1* transcripts were seen when *Steap3* was absent (Figure 6B). The absence of both *LcytB* and *Steap3* significantly increased *DMT1* expression beyond that seen in the absence of *LcytB* alone. Furthermore, *Tfrc1* transcripts were also upregulated in the absence of reductases *LcytB* and *Steap3*, but the loss of both was not additive for *Tfrc1*. Transcripts for the exporter ferroportin *Fpn1* were significantly decreased in the individual *LcytB* #2 and *Steap3* #2 mutants but, intriguingly, this effect was negated in the absence of both reductases. We do not have an explanation for this observation at this time. Our results indicate that loss of *LcytB* or *Steap3* results in limited bioavailable iron, which is sensed by the RAW264.7 macrophages and results in the upregulation of iron acquisition genes.

Transcript levels of *Steap3* and *LcytB* are altered upon exposure to pathogens

Macrophages are the major iron recycling cells in mammals, and when iron is abundant, macrophages also store iron in the cytosolic protein ferritin. In iron-limited conditions, macrophages recycle iron from stored intracellular ferritin.^{4,34} Macrophages are a key cell type in innate immunity, providing nutrients to tissues near sites of infection and limiting nutrient availability to opportunistic pathogens.^{35,36} Previous studies determined that *Steap3* transcripts were decreased when bone marrow-derived macrophages were exposed to the lipopolysaccharide present on many pathogens.²⁸ This finding suggests that macrophages respond to the presence of extracellular pathogens by signaling through MyD88 to limit iron release from the lysosome. To test whether *LcytB* expression is also altered by exposure to pathogens, we used the pathogenic *E. coli* strain UTI89.³⁷ We incubated WT RAW264.7 cells with or without UTI89 and examined *LcytB* and *Steap3* transcript levels. Both *LcytB* and *Steap3* transcripts were decreased by >50% upon exposure to UTI89 (Figure 7A). These results suggest that macrophages have an innate immune response to bacterial exposure to limit intracellular

iron release by reducing expression of reductases involved in iron release from lysosomes.

Loss of *LcytB* or *Steap3* improves proliferation of intracellular pathogen UTI89

Exposure to pathogens can cause cellular iron retention and sequestration in macrophages as a way to limit iron availability for extracellular pathogens.³⁸ Under these conditions, intracellular (or facultative intracellular) pathogens such as *E. coli*, *Salmonella typhimurium*, *Mycobacterium tuberculosis*, *Chlamydia psittaci*, and *Legionella pneumophila* are known to thrive.^{23,37,39,40} Organisms that live intracellularly in macrophages have evolved mechanisms to evade immune recognition and still have access to essential host intracellular iron. We questioned whether reductions in *LcytB* and/or *Steap3* affected the ability of pathogens to establish an intracellular niche. We infected WT RAW264.7, *LcytB* #2, *Steap3* #2, and *DKD* #2 cells with the pathogenic *E. coli* strain UTI89, which can reside in a vesicular compartment in macrophages,^{26,41} and we assessed invasion and proliferation. We did not observe any differences in bacterial adhesion that resulted from the loss of *LcytB* or *Steap3* (Figure 7B). At T_0 , 30 minutes after inoculation, loss of *LcytB* or *Steap3* led to increased intracellular titers of UTI89, although this was statistically significant only for the *LcytB* mutant (Figure 7C). Loss of both *LcytB* and *Steap3* did not have an additive effect. In overnight assays ($T_{O/N}$), the *LcytB* #2 and *Steap3* #2 both showed significantly increased numbers of bacteria compared with WT cells. In these longer assays, loss of both *LcytB* and *Steap3* had an additive effect, resulting in markedly higher intracellular bacterial titers than those observed in the WT macrophages (Figure 7D). Together, these results indicate important roles for the *LcytB* and *Steap3* reductases in limiting bacterial survival within macrophages. It is important to note that *E. coli* strains such as UTI89 can take up Fe^{3+} by siderophore secretion and by expressing bacterial reductases.^{42,43} Thus, Fe^{3+} retained in the endolysosomal system may be used by bacteria for proliferation. Our results support that limiting endosome and lysosome ferrireductase activity may provide a growth advantage to pathogens that survive in the endocytic pathway by retaining iron within endolysosomal membranes.

Discussion

Macrophages are key to iron recycling from red cells and iron release from stored ferritin. When iron demand is high, macrophages engulf ferritin through autophagy, ferritin is degraded in the lysosome, and iron is released as Fe^{3+} into the lysosomal lumen. All known mammalian iron transporters are Fe^{2+} transporters, including those present on the lysosome. Thus, iron export requires a lysosomal reductase to convert Fe^{3+} to Fe^{2+} that can then be exported to the cytosol for Fe^{2+} export back to plasma. Here, we provide evidence that the lysosomal protein *LcytB*, a predicted ferrireductase, is important in iron release from lysosomal-degraded ferritin in macrophages. Loss of *LcytB*, using CRISPR/Cas9 mutagenesis, reduced lysosomal iron export by about 50% in RAW264.7 macrophages. That there was still some iron export from the lysosome suggested that there was another reductase that could act in the absence of *LcytB*. We confirmed that reduction in *Steap3* decreased ferritin-released lysosomal iron export by approximately 50%, and the effects were additive in reducing iron export from the lysosome. Previous studies have reported that *LcytB* is the

predominant lysosomal reductase in Burkitt B cells, but that other B-cell lymphomas rely on Steap3.²⁵ This observation, together with results reported here, suggests that LcytB dependence may vary between cell types. We observed that Steap3 contributed to iron release from lysosomal localized ferritin and demonstrated that, similar to reports for DMT1,¹⁴ some Steap3 localized to the lysosome. In CF-loaded cells, only a small portion of Steap3 was found colocalized with Lamp2. One explanation for the small amount of colocalization is that Steap3 may be working at both the endosome and lysosome when lysosomal iron levels were increased. This possibility could occur through fusion of endosomes and lysosomes during cargo delivery (for review, see Luzio et al⁴⁴) where “kiss and run” between lysosomes and endosomes would provide rapid additional reductase activity to reduce iron and permit transport out of the endocytic pathway under high iron demand. In either case, we provide evidence that both LcytB and Steap3 contribute to lysosomal iron export.

Our *LcytB/Steap3* DKD cells still showed a small increase in the level of cytosolic ferritin after CF loading. Remaining iron export from the lysosome can be explained either by remaining LcytB or Steap3 activity or by the existence of another reductase that can function in the absence of LcytB and Steap3. It is also possible that there are reducing equivalents present in the lysosome that can convert Fe³⁺ to Fe²⁺, as suggested by La et al.¹⁴ We observed that *Steap2* and *Steap4* expression levels were increased in response to the loss of both LcytB and Steap3. Both Steap2 and Steap4 have been localized to the endocytic pathway,⁴⁵ and we predict that they can contribute the endolysosomal iron export under limited LcytB and Steap3 reductase activities. To determine whether Steap2 and Steap4 contribute to lysosomal iron recycling will require the generation of quadruple-mutant cells lines, which is beyond the scope of this study.

LcytB is predicted to be an ascorbate-dependent reductase in which ascorbate provides the electron to reduce Fe³⁺ to Fe²⁺.¹⁶ In our studies, incubation of RAW264.7 mouse macrophages with ascorbate did not alter intracellular ferritin levels upon CF loading, which is different from that observed in fibroblasts.²⁴ In addition, we were surprised to find that our *LcytB* mutants grown in the presence of ascorbate showed an increase in intracellular ferritin levels upon CF loading. Our results suggest that ascorbate is altering cellular iron homeostasis independent of LcytB-mediated lysosomal iron reduction. The addition of ascorbate to growth medium is complicated to interpret because (1) ascorbate may reduce media Fe³⁺ to Fe²⁺ that can then be transported through plasma membrane DMT1 into the cytosol resulting in increased cellular ferritin levels, (2) ascorbic acid has been reported to inhibit lysosomal autophagy of ferritin,⁴⁶ (3) ascorbate has been speculated to stabilize ferritin or increase ferritin synthesis,^{47,48} and (4) increasing ascorbate levels have been suggested to provide electron donors in the cytosol that can reduce ferritin iron from Fe³⁺ to Fe²⁺, allowing iron release directly into the cytosol.⁴⁹ In all of these cases, one might expect to see changes in macrophage ferritin levels independent of LcytB status. Future studies are required to tease out the consequences of altering cellular ascorbate levels and how ascorbate affects iron homeostasis in macrophages.

One prediction of loss of either LcytB or Steap3 is that whole-cell iron levels will change. Interestingly, we observed that loss of LcytB did not affect iron levels, whereas loss of Steap3 reduced amounts

of whole-cell iron by about 50%. We suggest that there were no changes in whole iron in LcytB-mutant cells because the iron becomes sequestered within the lysosome. The changes observed in Steap3-mutant cells may mean that RAW264.7 macrophages are highly dependent upon Steap3 for iron acquisition via Tfrc1-Tf(Fe)₂ uptake and Steap3-mediated endosomal reduction of Fe³⁺ to Fe²⁺ before export out of the endosome through DMT1. It was surprising to find that Mn and Cu levels were reduced upon loss of LcytB and Steap3, respectively. It has been shown that Steap3 can act as a Cu reductase³¹ and that Fe and Cu metabolism are tightly regulated.⁵⁰ Thus, Steap3 loss may reflect a decrease in Cu uptake through the Cu transporters Ctr1 and Ctr2.⁵¹⁻⁵⁴ We speculate that the change in Mn levels in LcytB-mutant cells may reflect competition for metal transport through DMT1 or other metal transporters (such as NRAMP1 or TRPML1), which are known to transport several different divalent metals.⁵⁵⁻⁵⁸ Why Mn is specifically reduced in the absence of LcytB remains to be determined. Perhaps our most intriguing finding was that loss of both LcytB and Steap3 restores normal levels of these metals within the whole cells. We observed that *DMT1* transcripts were upregulated about twofold by loss of both LcytB and Steap3 compared with loss of LcytB alone, whereas *Tfrc1* expression was not significantly altered in the absence of both LcytB and Steap3 in comparison with the single reductase deletions. These observations suggest that elevated DMT1 levels may allow for increased cellular Fe, Mn, and Cu uptake needed for cellular functions and survival. Further analysis of the uptake of these metals and their subcellular localization may provide additional insight into how LcytB and Steap3 impact the use and storage of metals by macrophages.

It is known that macrophages retain iron to sequester it away from extracellular pathogens.³⁸ Some pathogens have taken advantage of this to survive and acquire iron inside of macrophages. We found that UTI89, a uropathogenic *E. coli* strain, which can reside within a vesicular compartment in macrophages,^{26,37,41} persisted and proliferated better in our mutant lines *LcytB* #2, *Steap3* #2, and *DKD* #2 RAW264.7 macrophages. These observations support the hypothesis that there is more endolysosomal iron available for pathogen proliferation in the absence of LcytB. We and others have observed that Steap3 and LcytB expression is reduced in response to pathogen exposure.^{28,59} This suggests that these reductases may be part of the innate immune response in macrophages that limits nutrient bioavailability during infection. We speculate that these reductases may also contribute to macrophage-mediated iron delivery to the surrounding tissue environment. Future studies are focused on determining the contribution of LcytB to both innate immune regulation and macrophage function.

In conclusion, our studies have identified the reductases LcytB and Steap3 as important players in the conversion of Fe³⁺ to Fe²⁺ within the lysosome, allowing for Fe²⁺ export back to the macrophage cytosol. *Steap3* mutations have been identified in humans and result in microcytic anemia,⁶⁰ and the *Steap3* knockout mouse shows retention of iron in macrophages and anemia, although the levels are reduced by only approximately 60%.³⁰ These observations suggested that a reductase other than Steap3 is important for iron recycling and iron homeostasis. Here, we provide evidence that lysosomal LcytB acts as an additional macrophage reductase important in ferritin iron recycling. No known mutations in *LcytB* have been reported in humans, and future studies regarding the role of

LcytB in iron homeostasis in macrophages as well as other cell types are merited.

Acknowledgments

The authors thank Ben Gewurz for generously providing lentiviral constructs of WT and Y66A-mutant human *LcytB*, acknowledge the Cell Imaging Core for use of the Zeiss 700 confocal microscope at the University of Utah, and acknowledge Mike Bridge for assistance with confocal image acquisition and image processing.

This work is supported by grants from the National Institutes of Health, National Institute of Diabetes and Digestive and Kidney Diseases (NIDDK) (DK30534), by a U54 NIDDK-sponsored Center for Iron and Heme Disorders Pilot & Feasibility grant (U54DK110858) (D.M.W.), and by grants from the National Institute of Allergy and Infectious Diseases (AI095647) and the National Institute of General Medical Sciences (GM134331) (M.A.M.).

References

1. Ajioka RS, Phillips JD, Kushner JP. Biosynthesis of heme in mammals. *Biochim Biophys Acta*. 2006;1763(7):723-736.
2. Rawat S, Stemmler TL. Key players and their role during mitochondrial iron-sulfur cluster biosynthesis. *Chemistry*. 2011;17(3):746-753.
3. Gkouvatzos K, Papanikolaou G, Pantopoulos K. Regulation of iron transport and the role of transferrin. *Biochim Biophys Acta*. 2012;1820(3):188-202.
4. Ganz T. Macrophages and iron metabolism. *Microbiol Spectr*. 2016;4(5). <https://doi.org/10.1128/microbiolspec.MCHD-0037-2016>.
5. Bouhassira EE. Concise review: production of cultured red blood cells from stem cells. *Stem Cells Transl Med*. 2012;1(12):927-933.
6. White C, Yuan X, Schmidt PJ, et al. HRG1 is essential for heme transport from the phagolysosome of macrophages during erythrophagocytosis. *Cell Metab*. 2013;17(2):261-270.
7. Pek RH, Yuan X, Rietzschel N, et al. Hemozoin produced by mammals confers heme tolerance. *eLife*. 2019;8:e49503.
8. Linder MC. Mobilization of stored iron in mammals: a review. *Nutrients*. 2013;5(10):4022-4050.
9. Ward DM, Kaplan J. Ferroportin-mediated iron transport: expression and regulation. *Biochim Biophys Acta*. 2012;1823(9):1426-1433.
10. Dowdle WE, Nyfeler B, Nagel J, et al. Selective VPS34 inhibitor blocks autophagy and uncovers a role for NCOA4 in ferritin degradation and iron homeostasis in vivo. *Nat Cell Biol*. 2014;16(11):1069-1079.
11. Gryzik M, Srivastava A, Longhi G, et al. Expression and characterization of the ferritin binding domain of Nuclear Receptor Coactivator-4 (NCOA4). *Biochim Biophys Acta Gen Subj*. 2017;1861(11 pt A):2710-2716.
12. Mancias JD, Wang X, Gygi SP, Harper JW, Kimmelman AC. Quantitative proteomics identifies NCOA4 as the cargo receptor mediating ferritinophagy. *Nature*. 2014;509(7498):105-109.
13. Asano T, Komatsu M, Yamaguchi-Iwai Y, Ishikawa F, Mizushima N, Iwai K. Distinct mechanisms of ferritin delivery to lysosomes in iron-depleted and iron-replete cells. *Mol Cell Biol*. 2011;31(10):2040-2052.
14. La A, Nguyen T, Tran K, et al. Mobilization of iron from ferritin: new steps and details. *Metallomics*. 2018;10(1):154-168.
15. Dong XP, Cheng X, Mills E, et al. The type IV mucopolidiosis-associated protein TRPML1 is an endolysosomal iron release channel. *Nature*. 2008;455(7215):992-996.
16. Zhang DL, Su D, Bérczi A, Vargas A, Asard H. An ascorbate-reducible cytochrome b561 is localized in macrophage lysosomes. *Biochim Biophys Acta*. 2006;1760(12):1903-1913.
17. Verelst W, Asard H. A phylogenetic study of cytochrome b561 proteins. *Genome Biol*. 2003;4(6):R38.
18. McKie AT, Barrow D, Latunde-Dada GO, et al. An iron-regulated ferric reductase associated with the absorption of dietary iron. *Science*. 2001;291(5509):1755-1759.
19. Shatwell KP, Dancis A, Cross AR, Klausner RD, Segal AW. The FRE1 ferric reductase of *Saccharomyces cerevisiae* is a cytochrome b similar to that of NADPH oxidase. *J Biol Chem*. 1996;271(24):14240-14244.
20. Su D, Asard H. Three mammalian cytochromes b561 are ascorbate-dependent ferrireductases. *FEBS J*. 2006;273(16):3722-3734.
21. Weber RA, Yen FS, Nicholson SPV, et al. Maintaining iron homeostasis is the key role of lysosomal acidity for cell proliferation. *Mol Cell*. 2020;77(3):645-655.e7.

Authorship

Contribution: F.M. performed experiments, generated figures, and helped write the manuscript; B.A.F. designed and performed experiments and edited the manuscript; X.J. performed experiments and edited the manuscript; A.A.R. performed mutagenesis of pLcytB-GFP; M.A.M. designed experiments and edited the manuscript; and D.M.W. designed and performed experiments, generated figures, and helped write the manuscript.

Conflict-of-interest disclosure: The authors declare no competing financial interests.

ORCID profile: X.J., 0000-0002-3986-0687.

Correspondence: Diane M. Ward, Department of Pathology, University of Utah School of Medicine, 26 North Medical Dr, Room 621, Salt Lake City, UT 84132; e-mail: diane.mcveyward@path.utah.edu.

22. Ohgami RS, Campagna DR, Greer EL, et al. Identification of a ferrereductase required for efficient transferrin-dependent iron uptake in erythroid cells. *Nat Genet.* 2005;37(11):1264-1269.
23. Paradkar PN, De Domenico I, Durchfort N, Zohn I, Kaplan J, Ward DM. Iron depletion limits intracellular bacterial growth in macrophages. *Blood.* 2008;112(3):866-874.
24. Radisky DC, Kaplan J. Iron in cytosolic ferritin can be recycled through lysosomal degradation in human fibroblasts. *Biochem J.* 1998;336(pt 1):201-205.
25. Wang Z, Guo R, Trudeau SJ, et al. CYB561A3 is the key lysosomal iron reductase required for Burkitt B-cell growth and survival. *Blood.* 2021; 138(22):2216-2230.
26. Eto DS, Jones TA, Sundsbak JL, Mulvey MA. Integrin-mediated host cell invasion by type 1-piliated uropathogenic *Escherichia coli*. *PLoS Pathog.* 2007;3(7):e100.
27. Bailis W. CRISPR/Cas9 gene targeting in primary mouse bone marrow-derived macrophages. *Methods Mol Biol.* 2020;2097:223-230.
28. Zhang F, Tao Y, Zhang Z, et al. Metalloreductase Steap3 coordinates the regulation of iron homeostasis and inflammatory responses. *Haematologica.* 2012;97(12):1826-1835.
29. Blanc L, Papoin J, Debnath G, et al. Abnormal erythroid maturation leads to microcytic anemia in the TSAP6/Steap3 null mouse model. *Am J Hematol.* 2015;90(3):235-241.
30. Lambe T, Simpson RJ, Dawson S, et al. Identification of a Steap3 endosomal targeting motif essential for normal iron metabolism. *Blood.* 2009; 113(8):1805-1808.
31. Ohgami RS, Campagna DR, McDonald A, Fleming MD. The Steap proteins are metalloreductases. *Blood.* 2006;108(4):1388-1394.
32. Muckenthaler MU, Galy B, Hentze MW. Systemic iron homeostasis and the iron-responsive element/iron-regulatory protein (IRE/IRP) regulatory network. *Annu Rev Nutr.* 2008;28(1):197-213.
33. Knutson MD, Vafa MR, Haile DJ, Wessling-Resnick M. Iron loading and erythrophagocytosis increase ferroportin 1 (FPN1) expression in J774 macrophages. *Blood.* 2003;102(12):4191-4197.
34. Nairz M, Theurl I, Swirski FK, Weiss G. "Pumping iron"-how macrophages handle iron at the systemic, microenvironmental, and cellular levels. *Pflugers Arch.* 2017;469(3-4):397-418.
35. Nairz M, Theurl I, Ludwiczek S, et al. The co-ordinated regulation of iron homeostasis in murine macrophages limits the availability of iron for intracellular *Salmonella typhimurium*. *Cell Microbiol.* 2007;9(9):2126-2140.
36. Sukhbaatar N, Weichhart T. Iron regulation: macrophages in control. *Pharmaceuticals (Basel).* 2018;11(4):137.
37. Eto DS, Sundsbak JL, Mulvey MA. Actin-gated intracellular growth and resurgence of uropathogenic *Escherichia coli*. *Cell Microbiol.* 2006;8(4):704-717.
38. Cherayil BJ. The role of iron in the immune response to bacterial infection. *Immunol Res.* 2011;50(1):1-9.
39. Nix RN, Altschuler SE, Henson PM, Detweiler CS. Hemophagocytic macrophages harbor *Salmonella enterica* during persistent infection. *PLoS Pathog.* 2007;3(12):e193.
40. Olakanmi O, Schlesinger LS, Britigan BE. Hereditary hemochromatosis results in decreased iron acquisition and growth by *Mycobacterium tuberculosis* within human macrophages. *J Leukoc Biol.* 2007;81(1):195-204.
41. Baorto DM, Gao Z, Malaviya R, et al. Survival of FimH-expressing enterobacteria in macrophages relies on glycolipid traffic. *Nature.* 1997; 389(6651):636-639.
42. Koch D, Chan AC, Murphy ME, Lilie H, Grass G, Nies DH. Characterization of a dipartite iron uptake system from uropathogenic *Escherichia coli* strain F11. *J Biol Chem.* 2011;286(28):25317-25330.
43. Wilson BR, Bogdan AR, Miyazawa M, Hashimoto K, Tsuji Y. Siderophores in iron metabolism: from mechanism to therapy potential. *Trends Mol Med.* 2016;22(12):1077-1090.
44. Luzio JP, Pryor PR, Bright NA. Lysosomes: fusion and function. *Nat Rev Mol Cell Biol.* 2007;8(8):622-632.
45. Grunewald TG, Bach H, Cossarizza A, Matsumoto I. The STEAP protein family: versatile oxidoreductases and targets for cancer immunotherapy with overlapping and distinct cellular functions. *Biol Cell.* 2012;104(11):641-657.
46. Bridges KR. Ascorbic acid inhibits lysosomal autophagy of ferritin. *J Biol Chem.* 1987;262(30):14773-14778.
47. Bridges KR, Hoffman KE. The effects of ascorbic acid on the intracellular metabolism of iron and ferritin. *J Biol Chem.* 1986;261(30):14273-14277.
48. Richardson DR. Role of ceruloplasmin and ascorbate in cellular iron release. *J Lab Clin Med.* 1999;134(5):454-465.
49. Badu-Boateng C, Naftalin RJ. Ascorbate and ferritin interactions: consequences for iron release in vitro and in vivo and implications for inflammation. *Free Radic Biol Med.* 2019;133:75-87.
50. Knutson MD. Steap proteins: implications for iron and copper metabolism. *Nutr Rev.* 2007;65(7):335-340.
51. Nose Y, Wood LK, Kim BE, et al. Ctr1 is an apical copper transporter in mammalian intestinal epithelial cells in vivo that is controlled at the level of protein stability. *J Biol Chem.* 2010;285(42):32385-32392.
52. Öhrvik H, Nose Y, Wood LK, et al. Ctr2 regulates biogenesis of a cleaved form of mammalian Ctr1 metal transporter lacking the copper- and cisplatin-binding ecto-domain. *Proc Natl Acad Sci USA.* 2013;110(46):E4279-E4288.

53. White C, Kambe T, Fulcher YG, et al. Copper transport into the secretory pathway is regulated by oxygen in macrophages. *J Cell Sci.* 2009; 122(pt 9):1315-1321.
54. Achard ME, Stafford SL, Bokil NJ, et al. Copper redistribution in murine macrophages in response to Salmonella infection. *Biochem J.* 2012; 444(1):51-57.
55. Lin C, Zhang Z, Wang T, Chen C, Kang YJ. Copper uptake by DMT1: a compensatory mechanism for CTR1 deficiency in human umbilical vein endothelial cells. *Metallomics.* 2015;7(8):1285-1289.
56. Wolff NA, Garrick MD, Zhao L, Garrick LM, Ghio AJ, Thévenod F. A role for divalent metal transporter (DMT1) in mitochondrial uptake of iron and manganese. *Sci Rep.* 2018;8(1):211.
57. Dong XP, Wang X, Shen D, et al. Activating mutations of the TRPML1 channel revealed by proline-scanning mutagenesis. *J Biol Chem.* 2009; 284(46):32040-32052.
58. Jabado N, Jankowski A, Dougaparsad S, Picard V, Grinstein S, Gros P. Natural resistance to intracellular infections: natural resistance-associated macrophage protein 1 (Nramp1) functions as a pH-dependent manganese transporter at the phagosomal membrane. *J Exp Med.* 2000;192(9): 1237-1248.
59. Zhang J, Cheng Y, Duan M, Qi N, Liu J. Unveiling differentially expressed genes upon regulation of transcription factors in sepsis. *3 Biotech.* 2017; 7(1):46.
60. Grandchamp B, Hetet G, Kannengiesser C, et al. A novel type of congenital hypochromic anemia associated with a nonsense mutation in the STEAP3/TSAP6 gene. *Blood.* 2011;118(25):6660-6666.